Fluorescence Characteristics of Wholesome and Unwholesome Chicken Carcasses

MOON S. KIM,* YUD-REN CHEN, SUKWON KANG, INTAEK KIM, ALAN M. LEFCOURT, and MOONJOHN KIM

Instrumentation and Sensing Laboratory, Beltsville Agricultural Research Center, Agricultural Research Service, U.S. Department of Agriculture, Beltsville, Maryland 20705 (M.S.K., Y.-R.C., A.M.L.); Quality and Safety Evaluation Laboratory, National Institute of Agricultural Engineering, Rural Development Administration, Suwon, Gyeonggi-do, Korea (S.K.); Department of Communication Engineering, Myongji University, Yongin, Gyeonggi-do, Korea (I.K.); and Department of Diagnostic Radiology, University of Maryland Medicine, Baltimore, Maryland, 21201 (M.K.)

Each chicken carcass intended for U.S. consumers is mandated to be inspected by Food Safety and Inspection Service (FSIS) inspectors for its wholesomeness at the processing plants. Fluorescence responses of wholesome and unwholesome chicken carcasses were characterized and further evaluated for potential on-line applications for detection and classification of wholesome and unwholesome chicken carcasses. For this study, unwholesome chicken carcasses included cadaver and those with disease conditions such as airsacculitis and septicemia. Fluorescence characteristics from the epidermal layers in the breast areas of chicken carcasses were dynamic in nature. Emission peaks and ridges (maxima) were observed at 386, 444, 472, 512, and 554 nm and valleys (minima) were observed at 410, 460, 484, and 538 nm. One of the major factors affecting the line shapes of fluorescence responses from chicken carcass skin layers was absorption by hemoglobin. With the use of the normalized ratio spectra (NRS) approach, oxyhemoglobin was shown to be a major constituent in chicken carcasses affecting the fluorescence emission line shapes. Subtle line shape changes in the NRS also provided a qualitative means by which to assess the minute differences in oxy- and deoxyhemoglobin compositions perturbed by poultry diseases such as septicemia and airsacculitis. With the use of simple fluorescence band ratios as a multivariate model, wholesome and unwholesome chicken carcasses were correctly classified with 97.1% and 94.8% accuracies, respectively. On-line implementation of fluorescence techniques for the assessment of chicken carcass wholesomeness appears promising.

Index Headings: **Fluorescence; Chicken carcasses; Poultry disease; Food safety.**

INTRODUCTION

Poultry product consumption has been steadily increasing in the U.S. for the past several decades. Per capita consumption of chicken increased from 28.0 pounds in 1960 to 76.5 pounds in 2000, and is expected to reach over 90 pounds in 2006.[1] The number of chickens processed at federally inspected establishments was 8.5 billion birds in 2000. Chickens with infectious conditions (to humans) exist at the time of slaughter. Since 1959, U.S. law has required that each chicken intended for sale to U.S. consumers be inspected for wholesomeness by Food Safety and Inspection Service (FSIS) inspectors of the United States Department of Agriculture (USDA).[2] These inspectors manually inspect poultry carcasses and viscera on-line at processing plants. Unwholesome conditions include septicemia, ascites, airsacculitis, inflammatory, tumorous, and cadaver. The inspectors remove carcasses exhibiting these conditions; currently, carcasses with septicemia are condemned, while those with other conditions are removed from the processing lines for further evaluation/trimming.

In recent years, FSIS transformed its traditional inspection system to a Hazard-Analysis-and-Critical-Control-Point (HACCP) inspection system. Under this regime, FSIS inspectors still perform a bird-by-bird organoleptic examination, but FSIS also monitors a producer-run HACCP plan, which is developed by each plant and approved by FSIS. In addition, FSIS has started evaluating the division of responsibilities between government and processing plants (i.e., the HACCP-based Inspections Models Project).[3] Under this regime, there is a need to develop automated inspection systems that can detect carcasses with infectious conditions and also maintain high detection accuracies regardless of changes in carcasses due to variations in diet, growing condition, and variety. Such systems, placed strategically in the processing plants, can improve inspection speed, minimize human error and variability due to fatigue, improve the effectiveness of the federal inspection program, and ultimately increase productivity.[4] Spectral sensing techniques may allow measurements with such specificity. The USDA Instrumentation and Sensing Laboratory has been developing several automated systems using reflectance techniques in the visible (VIS) to near-infrared (NIR) regions of the spectrum to inspect chicken carcasses for wholesomeness.[5–8] For separation of wholesome and unwholesome chicken carcasses using the reflectance method, classification accuracies of low- to mid- 90% have been reported.

Another spectroscopic sensing method available is fluorescence. Animal tissues contain various compounds that emit fluorescence when excited with electromagnetic radiation in the ultraviolet (UV) to VIS regions.[9] The UV fluorescence emanates from proteins, while emissions in the blue-green regions of the spectrum have been linked to a myriad of aromatic compounds.[10–14] Fluorescence from intact biological samples is a complex interaction of many factors. One of the factors that affects the fluorescence responses of animal tissue is the presence of blood that exhibits strong absorption in the UV to visible regions of the spectrum.[14,15] In the food sciences, fluorescence sensing techniques have been applied mainly for quality assessments. Several studies have utilized autofluorescence from meat samples,[12–14,16,17] yet the technique has not been exploited for determination of wholesomeness for chicken carcasses. Objectives of this investigation are to characterize fluorescence properties of various chicken carcasses including wholesome, cadaver, and those affected by diseases such as airsacculitis and septicemia. Furthermore, the potential of fluorescence sensing techniques for on-line applications for detection and classification of wholesome and unwholesome chicken carcasses was investigated. Fluorescence measurements were acquired on breast area skin layers of intact chicken carcasses.

Received 17 November 2005; accepted 11 July 2006.
* Author to whom correspondence should be sent. E-mail: kimm@ba.ars.usda.gov.

0003-7028/06/6010-1210$2.00/0

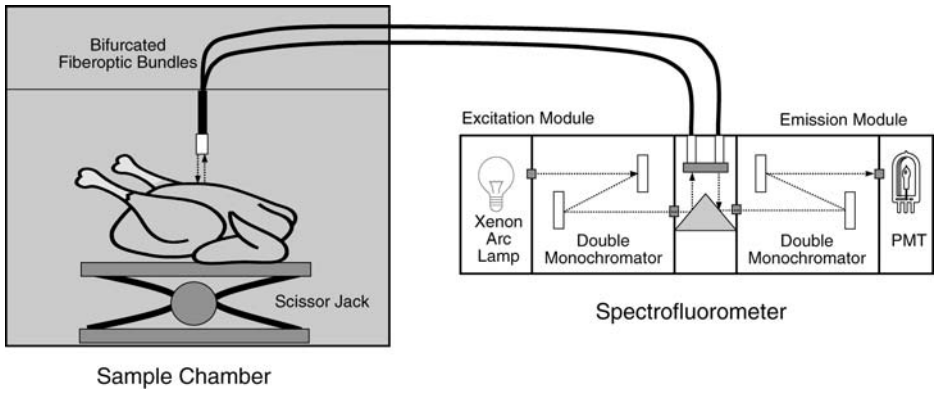

FIG. 1. Schematic illustration of the experimental setup and apparatus.

MATERIALS AND METHODS

Chicken Carcasses. A total of 130 broiler chicken carcasses were collected during eight visits to a nearby poultry processing plant (Allen Family Foods Inc., Cordova, MD) between October 2001 and June 2002. Chicken carcass samples consisted of 34 wholesome (normal), 29 cadaver, 28 septicemia, and 39 airsacculitis; the condition of each chicken sample was determined by one of two on-site FSIS veterinarians at the processing plant. All the samples were collected from the processing lines following the evisceration stage. Some of the septicemia carcasses were obtained from bins containing condemned carcasses, but only the most recently condemned samples from the top of the bins were collected in order to maintain consistency in carcass ages (approximately 30 minutes were spent for sample collection on each visit). The samples were tagged according to condition and placed in sealed plastic bags to minimize dehydration. Then the bags were placed in coolers, filled with ice to maintain approximately 4 °C, and transported to the Instrumentation and Sensing Laboratory. Within an hour of the transport (within 3 to 4 hours of sample collection at the plant), fluorescence measurements were conducted.

Cadaver carcasses are considered to be unwholesome due to improper bleeding during the slaughter process, and the resultant effects are not uniform throughout the breast areas. Fluorescence measurements were conducted from areas with reddish coloration caused by inadequate bleeding. Also, dark-purplish portions (bruises) of some cadaver carcasses were excluded in this study. The airsacculitis and septicemia samples ranged from mildly to severely affected. Carcasses evaluated as having both airsacculitis and septicemia were categorized by the more predominant symptoms manifested (generally considered to be septicemia samples per FSIS veterinarians). Septicemia, when severe, showed bluish skin discoloration and a waterlogged appearance compared to the white, yellowish skin tone exhibited by wholesome chicken carcasses.

Fluorescence Spectra. Fluorescence measurements for sample materials were performed using a commercial spectrofluorometer (Spex, Fluorolog III, Horiba Industries in Edison, NJ). It utilizes two 0.22 m additive dispersion, double grating scanning monochromators. One monochromator attached to a 450 W xenon arc lamp unit allows sample excitation from 220 to 700 nm. The second coupled with a photon counting photomultiplier tube (PMT) scans from 250 to 900 nm for fluorescence emission measurements. A bifurcated quartz fiber-optic attachment was used to measure spectra from samples (Fig. 1). The incident–detection side of the ferule (where fiber optics are bundled randomly) was positioned 2.5 cm above the sample surfaces at 90°; the effective area of illumination was approximately 2.0 cm in diameter. As illustrated in Fig. 1, a light-tight sample chamber (50 H × 40 W × 50 cm L) in conjunction with a height-adjustable scissor jack was used to eliminate ambient stray light and to accommodate various sample sizes, respectively.

Excitation and emission matrix (EEM) measurements were scanned from 350 to 650 nm with a 2.5 nm scan increment on the emission side and from 300 to 500 nm with a 5 nm scan increment on the excitation side. Acquisition of a complete EEM took approximately 20 min, and only three normal samples were scanned. For each chicken sample, emission spectra were acquired from 360 to 600 nm with a 2 nm scan increment and excitation wavelength fixed at 335 nm. Monochromators with slit-widths of 2 nm were used for both excitation and emission, and PMT integration time was kept at 0.2 s. For each chicken carcass, four independent fluorescence spectra were acquired from intact skin layers on breast areas and an average spectrum was calculated.

Based on the second-derivative spectra of the samples, wavelengths for emission peaks and ridges were determined and subjected to analysis of variance (ANOVA) and pairwise mean comparisons using SAS PROC MIX (Version 8.0, SAS Institute Inc., Cary, NC). Multivariate discriminant analysis/model cross-validation were also performed using the SAS procedures. Two-band ratio combinations of peak and valley wavelengths were subjected to the SAS PROC STEPDISC to sequentially identify the most significant ratio pairs (up to five) with respect to the disease categories. The best classification model/cross-validation, assuming classes exhibited normal distribution and using a linear discriminant function, was determined using the SAS PROC DISCRIM. Cross-validation of the classification model was based on the goodness of one-sample-out cross-validation. Classifications/validations for the four disease categories, and airsacculitis and septecimia combined as unwholesome, were performed.

RESULTS AND DISCUSSION

Fluorescence Responses. Representative fluorescence excitation and emission matrix (EEM) that depict fluorescence responses as a function of excitation and emission wavelengths are shown in Fig. 2 for normal chicken carcasses. The three-dimensional mesh plot (Fig. 2a) illustrates the complex nature of the fluorescence responses with several emission peaks and

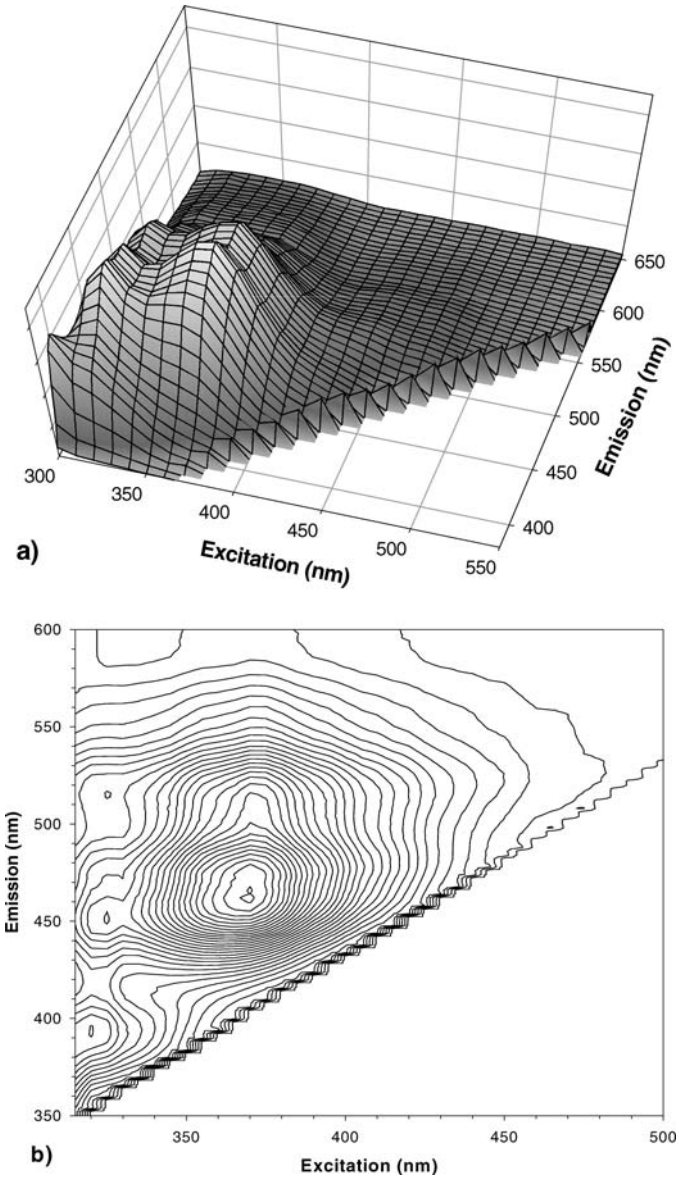

FIG. 2. Representative fluorescence excitation and emission matrix (EEM) obtained from intact normal chicken carcass skins. (**a**) Three-dimensional mesh plot and (**b**) contour plot.

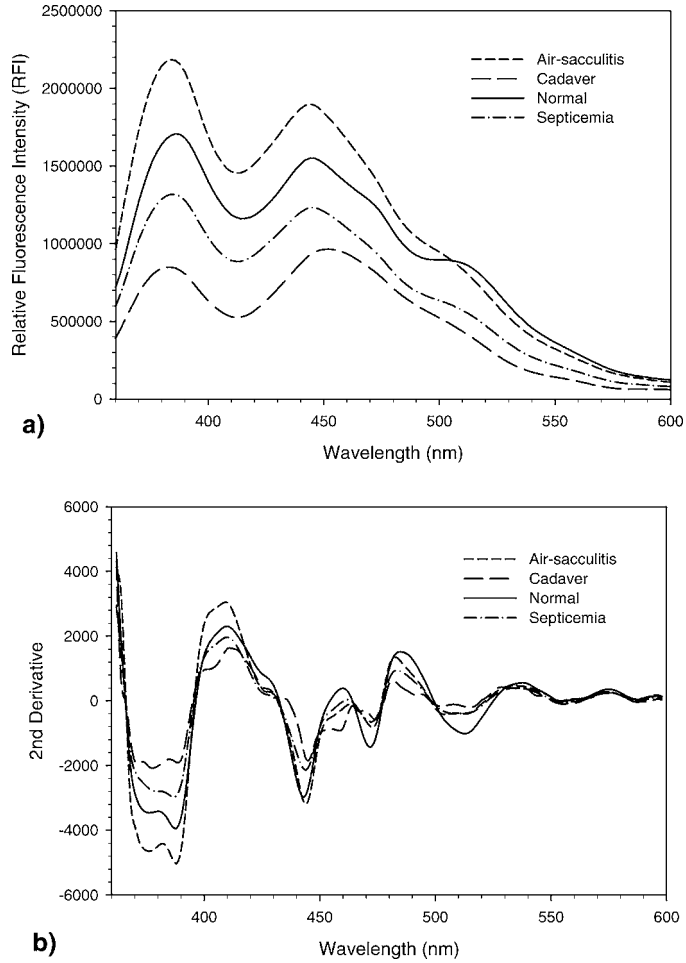

FIG. 3. (**a**) Mean fluorescence spectra of four chicken carcass categories, airsacculitis, cadaver, normal, and septicemia. Intensities are expressed in relative fluorescence intensity (RFI). (**b**) Mean second-derivative spectra obtained from individual fluorescence spectra of the four chicken carcass categories under investigation.

ridges (or shoulders) in the UV to visible regions of the spectrum. Several factors can affect the fluorescence response from optically thick (turbid) chicken breast skin. One factor is the distribution of the excitation light, dependent on the absorption and scattering characteristics of the excitation wavelength. Another is the fluorophore distribution, which varies at different depths within the tissue. A third factor is the total fluorescence emission from the surface of the skin, which is a function of the wavelength-specific absorption and scattering characteristics of the sample.

The contour plot (Fig. 2b) further illustrates excitation maximum (absorption maximum) wavelengths responsible for the fluorescence emissions. Relative intensities depend on the excitation wavelengths, but the wavelength location of the emission maximum (peak) is not dependent on the excitation wavelengths. Chicken skins exhibited emission characteristics consisting of a convolution of four emission peaks at approximately 390, 445, 470, and 515 nm. Note that because of the convoluted broad emissions, the wavelengths of the peaks and ridges (maxima) may shift slightly as intensities relative to each other change. Excitation near 315 nm was responsible for the emission maximum at near 390 nm. Two excitation maxima at approximately 325 and 370 nm were responsible for the emission maxima at 450 and 470, respectively. Although it is not clearly shown in Fig. 2b, a detailed evaluation of the EEM showed that there is an excitation maximum at 460 nm responsible for the emission maximum at 515 nm.

Mean fluorescence spectra expressed in relative fluorescence intensity (RFI) for the four chicken carcass categories, acquired from 360 nm to 600 nm with excitation at 335 nm, are shown in Fig. 3a. Upon evaluation of the EEM, 335 nm was chosen as the excitation wavelength for this investigation as it provided well-defined emission maxima from the UV to the blue-green region that can potentially be used for assessing chicken carcass conditions. For each chicken carcass category, second derivatives of individual sample spectra were also shown in Fig. 3b. Based on the evaluation of mean second-derivative spectra of normal samples, the emission peaks and ridges were determined to occur at 386, 444, 472, 512, and 554 nm, and valleys (minima) were observed at 410, 460, 484, 538, and 574

TABLE I. Mean relative fluorescence intensity values of the four chicken carcass categories at the emission maxima and minima. For each wavelength, means with different letters are significantly different according to the pairwise comparisons ($\alpha < 0.001$).

Emission maxima	386 nm	444 nm	472 nm	512 nm	554 nm
Normal	1753030 a	1604517 a	1305893 a	869967 a	334179 a
Airsacculitis	2102106 a	1867408 a	1409904 a	804142 a	294812 a
Septicemia	1355975 b	1260494 b	987635 b	557446 b	200060 b
Cadaver	839980 c	880969 c	761546 b	408742 c	130609 c
Emission minima	**410 nm**	**460 nm**	**484 nm**	**538 nm**	**574 nm**
Normal	1208955 a	1464107 a	1051062 a	484349 a	216090 a
Airsacculitis	1455449 a	1647023 a	1119251 a	424220 a	191190 a
Septicemia	903596 b	1146260 b	788440 b	284791 b	129617 b
Cadaver	523894 c	854552 b	618407 b	182610 c	80914 c

nm. The emission ridges and valleys between 450 and 550 nm were more pronounced in normal chicken spectrum and were the least evident in the cadaver spectrum.

Table I shows the mean RFI values and mean comparisons at the emission maxima and minima; mean comparisons were performed at the significance level (α) < 0.001. Beyond 500 nm, normal chickens had significantly higher RFI than airsacculitis. The mean trend reversal between normal and airsacculitis samples was the attributes of the emission ridge centered at 512 nm observed in the normal chickens. Consequently, RFI means for the four chicken carcass categories were significantly different at 538, 544, and 574 nm, where normal was the highest, followed by airsacculitis, septicemia, and cadaver, in that order.

Epidermal layers of a chicken carcass may contain many compounds that contribute to the significant fluorescence differences observed in the four chicken spectra.[12,13,15] At a given wavelength range, these may arise due to the differences in concentrations and physicochemical states (i.e., redox) of the fluorophores. Several investigators have suggested that the emission peak around 390 nm emanates from elastin and collagen, and attributed emission peaks in the 430 to 475 nm region to several aromatic compounds (i.e., membrane bound compounds, NAD(P)H).[12,13,15,18] Riboflavin, flavin mononecleotide (FMN), and flavin adenine dinucleotide (FAD) are known to exhibit emission maximum at around 515 nm. The observations from the EEM of chicken skins (Fig. 2) further supported the presence of these compounds. However, these may only account for a fraction of the fluorophores in chicken skin layers. Identification of compounds responsible for fluorescence emissions from such biological samples is very complex and is beyond the scope of this investigation.

Effects of Hemoglobin Absorption in Fluorescence Emission Spectra. Fluorescence from optically thick samples can also become strongly modulated by the wavelength-dependent absorption and scattering properties of the sample complex.[19,20] Thus, the presence of hemoglobin can reduce fluorescence emission throughout the wavelength range under investigation, as evidenced by observation of the cadaver spectrum that exhibited significantly lower RFIs compared to other chicken carcasses. It was also shown that hemoglobin absorption changes the line shape of fluorescence; fluorescence from optically thick tissue compared to that of a thin tissue section showed the appearance of a valley at 410 nm that corresponds to the Soret absorption band of hemoglobin.[14] Line shape modulations in association with oxyhemoglobin and deoxyhemoglobin absorptions can also be reflected in fluorescence throughout the visible region.[21]

To aid in the assessment of the fluorescence line shape changes by the absorption of hemoglobin in association with chicken carcass skins affected by physiological perturbations, a normalized ratio spectra (NRS) method was devised. Briefly, NRS is a simple transformation in that entire spectrum intensity values are normalized to that of a selected wavelength (scaled to an intensity value of 1), thus muting the spectral changes or the effects of the factor(s) modulating the intensity at that wavelength. When two normalized spectra are ratioed, relative spectral line changes caused by the factors other than the normalized are enhanced. It can also facilitate analysis of spectral data with large (wavelength dependent) variations (i.e., sample to sample or treatment to treatment) for visualization of small line shape changes that are not easily discernable. Some *a priori* knowledge of fluorescence emission (or absorbance) inherent to the sample of interest is useful for selecting the normalization wavelength.

Figures 4a and 4b show NRS, the line shape changes of samples relative to the normal and cadaver chicken carcasses, respectively. Note that individual chicken fluorescence spectra were normalized to 450 nm, and then ratio spectra (between chicken carcass category) were calculated using the normalized mean spectrum for each chicken carcass category. The blue band at 450 nm has relatively high and variable fluorescence emissions and is a relatively featureless region of hemoglobin absorption (Fig. 4c). Although the modulations were muted due to normalization at 450 nm, both Figs. 4a and 4b showed relatively small line shape changes in the 470 nm to 515 nm regions reflecting the effects of fluorophores. The NRS of the cadaver and normal (Figs. 4a and 4b, respectively) carcasses resembled and exhibited the three distinct absorption characteristics of oxyhemoglobin absorption peaks near 410, 535, and 575 nm shown in Fig. 4c. These observations clearly suggested that the reddish discoloration (due to improper bleeding) of cadaver carcasses compared to the normal is mainly due to the attributes of oxyhemoglobin.

In general, the line shapes of NRS of septicemia and airsacculitis also resembled that of the oxyhemoglobin. However, there existed subtle differences in the NRS of septicemia and airsacculitis when compared to that of the cadaver in that (1) 535 and 575 nm peaks were not as definitive, and (2) relatively small, blue-shifted peaks nears 400 nm were observed (Fig. 4a).

A study using fluorescence attenuation spectroscopy observed the disappearances of 535 and 575 nm peaks, and

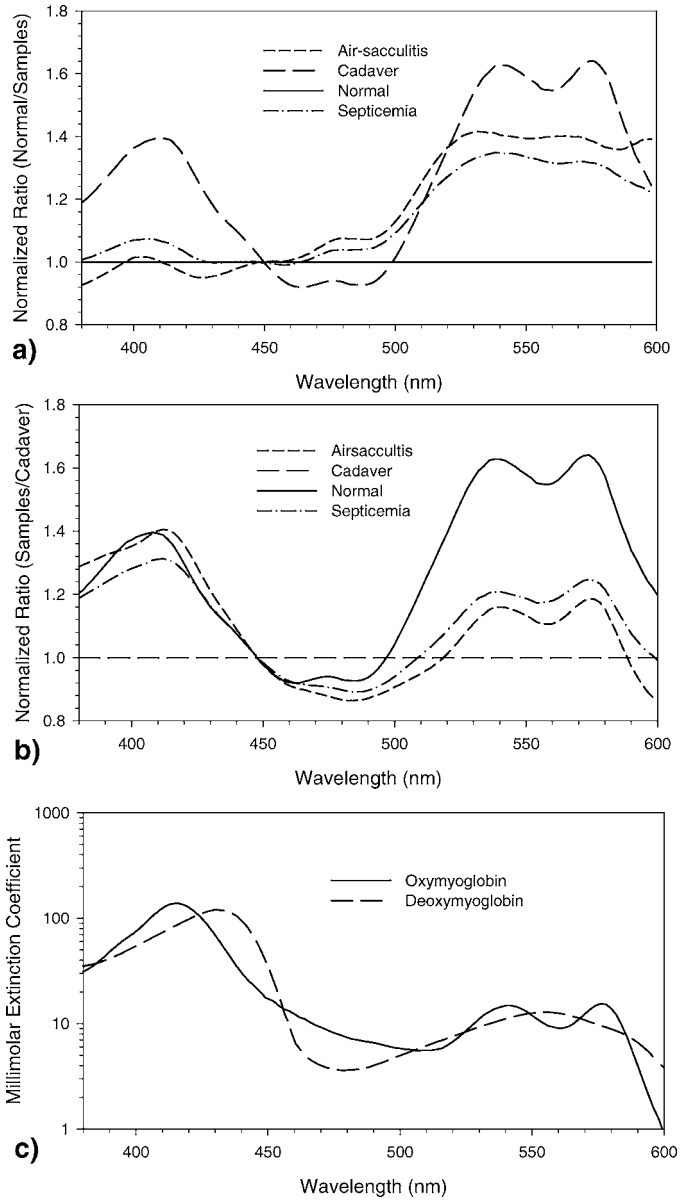

FIG. 4. Normalized ratio spectra of four chicken carcass categories: (**a**) normal was divided by other chicken carcass categories, and (**b**) airsacculitis, normal, and septicemia were divided by cadaver. The ratio spectra depict relative line shape changes with respect to (a) normal and (b) cadaver. (**c**) Absorption (extinction coefficients) spectra of oxyhemoglobin and deoxyhemoglobin (Redrawn with permission, Millar et al., 1994).[22]

disappearance of a small 400 nm peak as a result of increases in deoxygenated hemoglobin.[21] Furthermore, as shown in Fig. 4b, the absorption peaks around 410 nm for septicemia and airsacculitis were slightly red-shifted, and 360 nm relative to 410 nm intensities were higher when compared to that of the cadaver. These traits indicated a greater presence of deoxyhemoglobin for septicemia and airsacculitis.

The above observations suggested oxyhemoglobin as a major constituent in chicken carcasses (killed several hours prior to the measurements) affecting fluorescence emission line shapes. The subtle differences in the NRS for the septicemia and airsacculitis carcasses reflected the existence of greater fractions of deoxyhemoglobin than the normal and cadaver carcasses. In fact, septicemia results in relatively poor perfusion of oxygenated hemoglobin to peripheral tissue and increase in lactate production. Thus, there is relative tissue hypoperfusion resulting in relatively higher deoxyhemoglobin levels. Septicemia may also result in leaky capillary endothelium that contributes to the discoloration and textural differences on skins due to edema in the interstitial space compared to the normal. Airsacculitis causes poor oxygenation of hemoglobin and results in relatively high deoxyhemoglobin levels. Further research is needed to quantitatively assess compositions of hemoglobin derivatives in wholesome and unwholesome chicken carcass skin layers.

The fluorescence responses (line shape changes) demonstrated minute differences in oxy- and deoxyhemoglobin compositions perturbed by the poultry diseases. This implies that a method to assess the compositions of hemoglobin derivatives can also be used to determine the diseased carcasses. There exist multispectral spectrophotometric (i.e., absorption based) methods to assess hemoglobin derivatives, but uses are restricted to a controlled environment (i.e., *in vitro*) and sensitivity may be restricted for small changes.[23,24] Because of the high dependency of the fluorescence line shape modulations to absorption changes in hemoglobin derivatives, the fluorescence NRS technique can be refined to assess hemoglobin derivatives quantitatively. For instance, with the use of a background material that exhibits a broad fluorescence emission in the blue-green regions, fluorescence-NRS (normalized at the peak emission wavelength) of a smear of blood on the background material and background material itself will provide line shape changes only affected by relative absorption by the blood sample. Fluorescence measurements can be achieved in ambient light conditions with the use of a readily available laser-induced fluorescence sensor system.[25,26] Furthermore, the current reflectance-based, on-line automated inspection system is positioned on the kill line after bleeding and defeathering at the processing plants. Fluorescence techniques can potentially be used as an early detection tool, positioned immediately following the slaughter to assess the composition of hemoglobin derivatives. Identification and removal of unwholesome chicken carcasses at the very beginning stage of the processing has economical implications such as more efficient use of the processing lines and conservation of resources (i.e., water and fuel).

Detection of Wholesome and Unwholesome Chicken Carcasses. For applications of fluorescence to determine the wholesomeness of chicken carcasses, the sensitive nature of fluorescence can be both good and bad. It is sensitive in that physiological responses to diseases (subtle changes in biological entities) depicted in the epidermal layers of chicken carcasses can provide information necessary to be used to potentially determine wholesomeness. However, moving samples in the processing plant environment may introduce measurement errors (e.g., sensor to target distance, light source variation) that are not typically encountered in a controlled laboratory. The end results can be reflected as highly variable intensity responses. Hence, the use of fluorescence intensities alone may not be ideal for assessing wholesomeness of chicken carcasses on-line. One of the simplest methods to overcome the high variations in fluorescence responses associated with the on-line implementation is the use of ratios of two spectral bands. For this investigation, two band ratios of the emission minima and maxima were considered.

Classification cross-validations were performed using the

TABLE II. Summary of cross-validation results for classification of four chicken carcass categories: airsacculitis, cadaver, normal, and septicemia. Fluorescence band ratios, F512/F538, F460/F472, F472/F484, F538/F574, and F386/F538, were the inputs used for classification model.

	Assigned category				
Actual category	Airsacculitis	Cadaver	Normal	Septicemia	Total
Airsacculitis	25 (64.1)	0 (0.0)	2 (5.1)	12 (30.8)	39
Cadaver	0 (0.0)	28 (96.6)	0 (0.0)	1 (3.4)	29
Normal	1 (2.9)	0 (0.0)	33 (97.1)	0 (0.0)	34
Septicemia	8 (28.6)	1 (3.6)	2 (7.1)	17 (60.7)	28
Total	34	29	37	30	130

TABLE III. Summary of cross-validation results for classification of three chicken carcass categories: diseases (airsacculitis and septicemia), cadaver, and normal. Fluorescence band ratios, F538/F484, F472/F460, F574/F472, F574/F512, and F512/F460, were the inputs used for classification model.

	Assigned category			
Actual category	Diseases	Cadaver	Normal	Total
Diseases	63 (94.0)	1 (1.5)	3 (4.5)	67
Cadaver	2 (6.9)	27 (93.1)	0 (0.0)	29
Normal	1 (2.9)	0 (0.0)	33 (97.1)	34
Total	66	28	36	130

five best ratios selected (by the STEPDISC procedure) as model inputs. Results using individual spectral bands (RFI values) as the model inputs were slightly worse than those of the two band ratios, and are not discussed for brevity. Table II shows the cross-validation results of the multivariate discriminant analysis for the four chicken categories. The models were inadequate for discriminating the individual disease categories in that significant portions of airsacculitis and septicemia samples, 35.9% and 39.3%, respectively, were misclassified. However, the majority of the misclassifications were due to airsacculitis being classified as septicemia (30.8%) or vise versa (e.g., 28.6%). Samples in those disease categories exhibited symptoms ranging from mild to severe, with some carcasses having both disease conditions, which may explain the overlaps. The NRS also exhibited similar line shape modulations for the two disease categories. For cadaver and normal carcasses, the model correctly identified both with approximately 97% accuracies.

When the two disease categories were combined as a single category, the cross-validation classification accuracies markedly improved (Table III). The disease, cadaver, and normal carcasses were properly assigned to the categories with 94.0%, 93.1%, and 97.1% accuracies, respectively. Only 4.5% of the disease category and none of the cadaver were misclassified as normal. The classification results for the normal carcasses were consistent and only one normal chicken, accounting for 2.9%, was misclassified as disease category. When fluorescence ratio models were further evaluated for two classes, with one as wholesome (normal) and all other categories combined as unwholesome, chicken carcasses were correctly categorized with 97.1% and 94.8% accuracies, respectively. These results are very promising and also remarkable when considering that the samples encompassed a 9-month span of growth conditions. With the use of simple fluorescence band ratios, results from this investigation are analogous to the reflectance method currently being pursued for real time, on-line implementation at the chicken processing plants.

CONCLUSION

Using a commercial spectrofluorometer, fluorescence responses from intact epidermal layers on chicken breast areas were characterized for chicken carcass samples in four categories: normal, airsacculitis, septicemia, and cadaver. Fluorescence emission peaks and ridges (maxima) were observed at 386, 444, 472, 512, and 554 nm and valleys (minima) were observed at 410, 460, 484, and 538 nm. One of the major factors affecting the line shapes of fluorescence responses from chicken carcass skin layers was absorption by hemoglobin. A normalized ratio spectra (NRS) approach was devised, through which oxyhemoglobin was demonstrated to be a major constituent in the skin layers of chicken carcasses affecting the fluorescence emission line shapes. A subtle line shape change in the NRS provided a qualitative means to assess the minute differences in oxy- and deoxyhemoglobin compositions perturbed by poultry diseases such as septicemia and airsacculitis.

With the use of simple fluorescence band ratios, wholesome (normal) and unwholesome chicken carcasses were correctly classified with 97.1% and 94.8% accuracies, respectively. The results from this investigation are analogous to the reflectance measurements currently being pursued for real-time, on-line implementation at the chicken processing plants. On-line implementation of fluorescence techniques for the assessment of chicken carcass wholesomeness appears promising. Further detailed biochemical research is needed to identify compounds responsible for the fluorescence emission from epidermal layers of chicken carcasses.

Ultimately, on-line fluorescence measurement can be accomplished with the use of laser-induced fluorescence (LIF) techniques. A high intensity, short pulse laser coupled to a gated detection device can provide a rapid means to acquire fluorescence in ambient light conditions. Such a system capable of multispectral LIF imaging has already been developed by the researchers at the ISL, USDA.[26] This investigation is in an earlier stage in terms of evaluating the feasibility of fluorescence techniques for the assessment of chicken carcass wholesomeness. Future work will consist of incorporation of more disease categories and samples and implementation of a LIF-based system in on-line settings to further demonstrate the versatility of fluorescence sensing in food safety inspection. We also plan to further evaluate fluorescence NRS and develop quantitative models to assess fluorescence line shape changes in association with disease conditions and composition of hemoglobin derivatives.

ACKNOWLEDGMENTS

The authors would like to thank Ms. Diane Chan of ARS, USDA, and Mr. Frank Gwozdz of FSIS, USDA, for helping us in sample collection and transportation. We also extend our appreciation to Ms. Diane Chan for reviewing the paper. Company and product names are used for clarity and do not imply any endorsement by the USDA to the exclusion of other comparable products.

1. National Chicken Council Statistics, http://www.nationalchickencouncil.com/statistics/ (accessed 2004).
2. USDA. *Poultry Inspection Flier* (USDA, FSIS, Washington, D.C., 1989).
3. K. Chao, Y. R. Chen, and D. E. Chan, Appl. Eng. Agric. **19,** 453 (2003).
4. Y. R. Chen, K. Chao, W. R. Hruschka, and Y. Liu, "Optics in Agriculture 1990–2000", J. A. DeShazer and G. E. Meyer, Eds. SPIE-Crit. Rev. **80,** 140 (2001).
5. Y. R. Chen, R. W. Huffman, B. Park, and M. Nguyen, Appl. Spectrosc. **50,** 910 (1996).
6. Y. R. Chen, R. W. Huffman, M. Nguyen, and B. Park, J. Food Proc. Eng. **21,** 33 (1998).
7. B. Park, Y. R. Chen, and M. Nguyen, J. Agric. Eng. Res. **69,** 351 (1998).
8. B. Park, K. C. Lawrence, W. R. Windham, Y. R. Chen, and K. Chao, Comp. Elec. Agric. **33,** 219 (2002).
9. M. S. Kim, A. M. Lefcourt, and Y. R. Chen, J. Food Protect. **66,** 1198 (2003).
10. P. J. Harris and R. D. Hartley, Nature (London) **259,** 508 (1976).
11. E. W. Chappelle, J. E. McMurtrey, and M. S. Kim, Remote Sens. Environ. **36,** 213 (1991).
12. H. J. Swatland and S. Barbut, Int. J. Food Sci. Technol. **26,** 373 (1991).
13. J. P. Wold and K. Kvaal, Appl. Spectrosc. **54,** 900 (2000).
14. J. P. Wold, F. Lundby, and B. Egelandsdal, J. Food Sci. **64,** 377 (1999).
15. A. J. Durkin, S. Jaikumar, N. Ramanujam, and R. Richards-Kortum, Appl. Opt. **33,** 414 (1994).
16. S. G. Kong, Y. R. Chen, I. Kim, and M. S. Kim, Appl. Opt. **43,** 824 (2004).
17. I. Kim, M. S. Kim, Y. R. Chen, and S. G. Kong, Trans. ASAE **47,** 1785 (2004).
18. N. Ramanujam, "Fluorescence Spectroscopy In Vivo", in *Encyclopedia of Analytical Chemistry*, R. A. Meyers, Ed. (John Wiley and Sons Ltd, Chichester, 2000), pp. 20–56.
19. M. S. Kim, J. E. McMurtrey, C. L. Mulchi, C. S. T. Daughtry, and E. W. Chappelle, Y. R. Chem. Appl. Opt. **40,** 157 (2001).
20. C. Nrusingh, S. Gupta, N. Ghosh, and A. Pradhan, Opt. Express **11,** 3320 (2003).
21. R. E. N. Shehada, V. Z. Marmarelis, H. N. Mansour, and W. S. Grundfest, IEEE Trans. Biomed. Eng. **47,** 301 (2000).
22. S. J. Millar, B. W. Moss, and H. H. Stevenson, Meat Sci. **94,** 277 (1994).
23. W. G. Zijistra, A. Buursma, and A. Zwart, Clin. Chem. **34,** 149 (1988).
24. J. J. Mahoney, H. J. Vreman, D. K. Stevenson, and A. L. Van Kessel, Clin. Chem. **39,** 1693 (1993).
25. V. Tassetti, A. Hajri, M. Sowinska, S. Evrard, F. Heisel, L. Q. Cheng, J. A. Mieh, J. Marescaux, and M. Aprahamian, Photochem. Photobiol. **65,** 997 (1997).
26. M. S. Kim, A. M. Lefcourt, and Y. R. Chen, Appl. Opt. **42,** 3927 (2003).